

Neutron Resonance Measurements of Ag, Ta, and U^{238} †

R. G. FLUHARTY, F. B. SIMPSON, AND O. D. SIMPSON

Phillips Petroleum Company, Atomic Energy Division, Idaho Falls, Idaho

(Received January 23, 1956; revised version received June 4, 1956)

Transmission measurements of Ag, Ta, and U^{238} cross sections have been made with a resolution of 0.17 to 0.05 $\mu\text{sec}/\text{meter}$ and resonance parameters are presented in the energy region from 10 ev to roughly 300 ev. A brief description of the materials testing reactor fast chopper and its performance characteristics is included, and the resolution is demonstrated by resolving new resonances in Ta. Area analysis methods have been used with the primary objective being to determine values of $\bar{\Gamma}_n^0/D$. The values obtained are: Ag^{107} , $(0.40 \pm 0.16) \times 10^{-4}$; Ag^{109} , $(0.82 \pm 0.4) \times 10^{-4}$; Ta^{181} , $(1.7 \pm 0.3) \times 10^{-4}$; and U^{238} , $(1.55 \pm 0.5) \times 10^{-4}$. These results agree reasonably well with values previously reported.

I. INTRODUCTION

THE application of neutron time-of-flight spectrometers to the study of levels in the compound nucleus in the energy region slightly above neutron binding energies is yielding important information about details of these levels. Analysis procedures useful for total cross section measurements made with time-of-flight instruments have been developed at several laboratories.¹⁻⁴ Over the past few years, these methods have yielded sufficient data to show trends in the behavior of the various resonance parameters as functions of the number of nuclear particles. In particular, information⁵⁻⁷ about the ratio $\bar{\Gamma}_n^0/D$ can be compared with theoretical predictions.

The MTR fast chopper was constructed to utilize the high neutron flux available from the Materials Testing Reactor (MTR).⁸ Since a similar chopper in operation at Brookhaven National Laboratories (BNL) has been described previously,^{1,2} the description of the chopper itself will be limited to brief discussions of various component variations. The neutron source of the MTR chopper is different, so the response of the total instrument will be discussed at greater length.

The total neutron cross section of Ag, Ta, and U^{238} have been investigated in the neutron energy region from 10 to 3600 ev with the MTR fast chopper. In order to test the operation of the chopper, two standards and an unknown were measured. Ag and U^{238} were selected for the standards and Ta for the unknown since no recent high-resolution measurements of its cross section existed. Due to improved resolution, additional information about all three has been obtained.

† Work carried out under contract with the U. S. Atomic Energy Commission.

¹ Seidl, Hughes, Palevsky, Levin, Kato, and Sjöstrand, *Phys. Rev.* **95**, 476 (1954).

² F. G. P. Seidl, Brookhaven National Laboratory Report BNL-278 (5-46), 1954 (unpublished).

³ Melkonian, Havens, and Rainwater, *Phys. Rev.* **92**, 772 (1953).

⁴ Sailor, Landon, and Foote, *Phys. Rev.* **91**, 53 (1953).

⁵ Carter, Harvey, Hughes, and Pilcher, *Phys. Rev.* **96**, 113 (1954).

⁶ Harvey, Hughes, Carter, and Pilcher, *Phys. Rev.* **99**, 10 (1955).

⁷ R. Cote and L. M. Bollinger, *Phys. Rev.* **98**, 1162(A) (1955).

⁸ J. R. Huffman, *Nucleonics* **12**, No. 4, 21 (1954).

The primary objective of these measurements has been to determine $\bar{\Gamma}_n^0/D$, the ratio of the average reduced scattering width to level spacing per spin state, and thus emphasis has been placed upon determining $\bar{\Gamma}_n^0$ and D . Other factors of interest such as the resonance absorption width, peak cross sections, and potential scattering have also been determined.

II. APPARATUS

A schematic diagram of the fast chopper time-of-flight spectrometer^{9,10} is shown in Fig. 1. The source of neutrons is the HB-6 horizontal beam hole in the MTR.⁸ Aside from minor modifications, the MTR chopper is the same design as the chopper in operation at BNL.² The number of neutrons per unit time during the burst varies with time to give a triangular distribution which has a calculated full width at half-maximum of 1.6 μsec at 6000 rpm. The MTR instrument uses a light pulse timing system which traverses the rotor at 45° to the neutron beam. Use of the same path as the neutrons, which would give exact timing, is limited

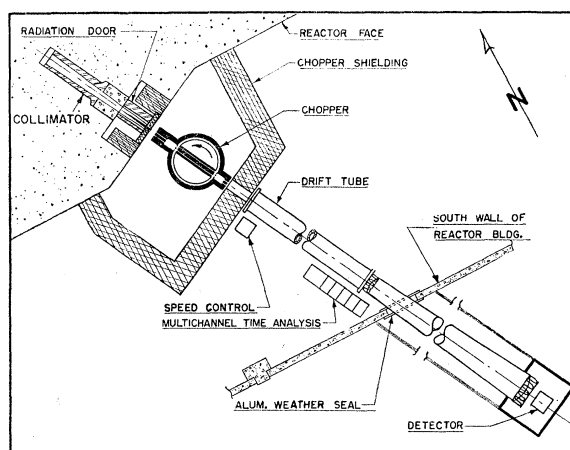


FIG. 1. A schematic diagram of the MTR fast-chopper time-of-flight neutron spectrometer. The drawing is not to scale and details have been simplified for clarity.

⁹ R. G. Fluharty, *Phys. Rev.* **95**, 609(A) (1954).

¹⁰ Fluharty, Simpson, and Simpson, U. S. Atomic Energy Commission Report IDO-16164, 1956 (unpublished).

since the quartz windows become opaque from radiation. The direct beam path is used for calibration of the 45° light system.

Neutron flight paths of 16, 30, and 45 meters have been used, and provisions have been made for a 60-meter flight path. To reduce air scattering, the neutrons pass from the chopper to the detector through "drift tubes" filled with He at atmospheric pressure.

Approximately 50 enriched BF_3 proportional counters are being used as a detector at the present time. A jitter of $0.5 \mu\text{sec}$ has been measured for these counters.¹¹

The timing circuit¹² records the neutrons in 100 equal-time channels. This circuit has a resolution or detection time of about 3–5 μsec . Thus, many detector pulses per burst can be recorded. Channel widths of $\frac{1}{2}$, 1, and 5 μsec have been used.

III. OPERATIONAL CHARACTERISTICS

The total open-beam spectrum at 30 meters as a function of time is shown in Fig. 2 by curve B. The resonance neutron spectrum is shown by curve A. The dips in the resonance spectrum are mostly due to Mn in the $2S$ aluminum windows in the collimator, drift tube, and detector. The source surface which is being used has a flux of 1×10^{14} thermal neutrons/cm² sec, and the expected resonance to thermal flux ratio is 1/31. The number of resonance neutrons passed by the rotor for each burst is 2.5 ± 0.5 neutrons per ev at 1 ev based upon both the observed counting rates and counter efficiency and calculated from the reactor flux.

Figure 3 shows the background with the various fractional parts indicated by the labeled lines. The

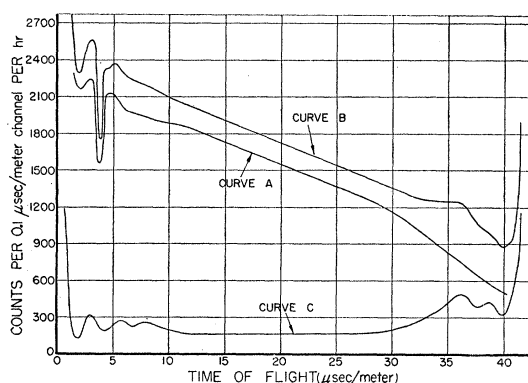


FIG. 2. The MTR fast-chopper spectrum at 30 meters. Curve A shows the resonance spectrum (without sample), curve B the total detector counting rate, and curve C the difference, $B-A$, or the total background. The "open beam" curve shows an E^{-1} spectrum modified by the chopper cutoff with structure due to various materials in the beam collimation system. At 30 meters "overlap" neutrons, those from a previous burst, are indicated since curve A does not drop to zero.

¹¹ O. D. Simpson, Phys. Rev. **95**, 600(A) (1954); R. G. Fluharty and O. D. Simpson, U. S. Atomic Energy Commission Report IDO-16110, 1954 (unpublished).

¹² D. R. deBoisblanc and K. A. McCollom, Phys. Rev. **95**, 609(A) (1954) and U. S. Atomic Energy Commission Report IDO-16159, 1954 (unpublished).

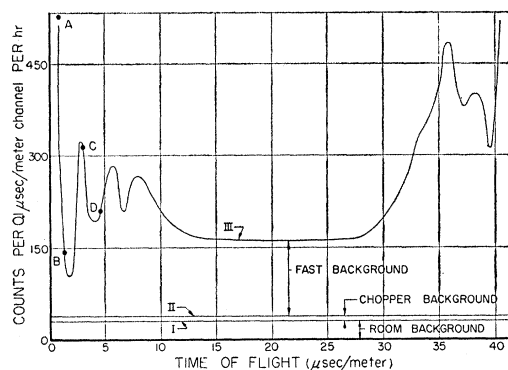


FIG. 3. The MTR fast-chopper background with a breakdown into its various parts. When the two constant backgrounds, curve II (the sum of the chopper and room backgrounds), are subtracted out, a prompt fast neutron background is found which has structure due to the variations in rotor thickness with angle or time. The capital letters correspond to the neutron paths labeled in Fig. 6. The "overlap" background is not included.

total background is obtained by measuring the total counting rate as a function of the rotor angle with the rotor static. A duty cycle conversion is made to the corresponding time-angle position.¹⁰ A boron filter is placed in front of the detector to reduce the general background and also to absorb the few thermal neutrons which leak through the rotor.

The measured structure in the background is caused by changes in the rotor thickness as seen by the high flux of fast neutrons from the MTR. The BNL fast-chopper time-of-flight spectrometer does not show this structure in the background because of the fast-neutron component of its beam is smaller. The MTR beam comes directly from a highly concentrated enriched fuel source with 6 in. of Be between the open collimation system and the fuel.

The time resolution function is similar to that described by Seidl *et al.*¹ However, in convoluting the various time functions, a measured value of counter "jitter"¹¹ has been used, and the detector lengths are different. The experimental transmissions for a thin sample of Ag at the 16-ev and 72-ev resonances are shown in Fig. 4 by the plotted points. The calculated transmission convoluted with the resolution function is given by the solid curve. The parameters given in Table I were used for the calculation.

Figure 5 is a curve of the over-all instrument resolution (full width at half-maximum) as a function of energy calculated for a detector length of 3 in. at 30 meters. This minimum detector length was chosen since time delays are used between groups of counters where different groups are located at slightly different distances along the flight path.¹³

The timing uncertainty can be reduced to about 0.5 μsec , but in the case of many individual resonances, the timing was not known that accurately. The timing

¹³ Simpson, Fluharty, and McClellan (to be published).

TABLE I. Parameters for resonances measured in Ag by MTR fast chopper. The $1/g$ factor is assumed to be 2, and Δ is the Doppler width of the level. Errors in individual parameters are estimates of accuracy and are taken to about 3 times as large as the precision associated with the measurements. ($1 \text{ mv} = 10^{-3} \text{ ev}$.)

E_0 (ev)	Isotope	$(1/n) \times 10^{24}$ cm^2/atom	Δ (ev)	Area (ev)	σ_0 (kb)	$g\Gamma_n$ (mv)	Γ_γ (mv)	Γ_n^0 (mv)
16.6 ± 0.2	107	52.36	0.125	2.01 ± 0.10	2.65 ± 0.66	2.6 ± 0.3	151 ± 23	1.3 ± 0.07
		2065		0.26 ± 0.02				
30.8 ± 0.3	109	26.53	0.172	2.7 ± 0.5	3.53 ± 0.64	5.45 ± 0.82	121 ± 13	2.0 ± 0.3
		2184		0.27 ± 0.10				
40.7 ± 0.6	109	2184	0.198	0.15 ± 0.03		3.5 ± 0.8	134^a	1.1 ± 0.13
42.4 ± 0.6	107	2065	0.202	0.17 ± 0.03		4.0 ± 0.8	135^a	1.23 ± 0.25
45.2 ± 0.6	107	185	0.202	0.33 ± 0.033		0.85 ± 0.13	135^a	0.25 ± 0.04
52.2 ± 0.6	107	184.7	0.216	1.58 ± 0.08	6.38 ± 1.38	17.2 ± 1.9	112 ± 24	3.17 ± 0.35^b
		2025		0.47 ± 0.035				
56.1 ± 2.0	109	195.3	0.224	1.18 ± 0.06	1.31 ± 0.54	6.81 ± 1.5	216 ± 85	3.63 ± 0.80^c
		2184		0.21 ± 0.05				
72.2 ± 2.0	109	195.3	0.262	1.41 ± 0.07	8.51 ± 1.87	22.3 ± 4.9	65 ± 35	3.47 ± 0.76^b
		2184		0.44 ± 0.09				
89.6 ± 2.4	109	195.3	0.277	0.49 ± 0.09		2.8 ± 0.6	134^a	0.59 ± 0.12
136 ± 5		190	0.36	2.49 ± 0.37		62 ± 11	134^a	10.6 ± 1.9
147 ± 5		190	0.38	1.40 ± 0.35		20 ± 9	134^a	3.4 ± 1.5
176 ± 6		190	0.41	3.28 ± 0.66		107 ± 34	134^a	16.1 ± 5.1
206 ± 9		190	0.45	1.03 ± 0.52		15 ± 8	134^a	2.1 ± 1.1
215 ± 9		190	0.45	1.28 ± 0.66		107 ± 34	134^a	3.0 ± 1.8
251 ± 11		53.8	0.49	9.68 ± 1.45		243 ± 73	134^a	30.6 ± 9.2
316 ± 16		53.8	0.55	6.44 ± 1.29		166 ± 58	134^a	18.7 ± 6.5

^a Assuming $\bar{\Gamma}_\gamma = 135 \pm 17 \text{ mv}$ for Ag^{107} and $\bar{\Gamma}_\gamma = 134 \pm 40 \text{ mv}$ for Ag^{109} .

^b Data indicates $g = \frac{1}{2}$.

^c Data indicate $g = \frac{1}{2}$.

uncertainty is implied in the energy error that is assigned to an individual resonance.

IV. ANALYSIS METHODS AND INTERPRETATION

Transmission and area analysis procedures have been used with the main objective being to determine the ratio of the average resonance scattering width to level spacing $\bar{\Gamma}_n^0/D$.^{1,3} Values have also been calculated for the potential scattering cross section.

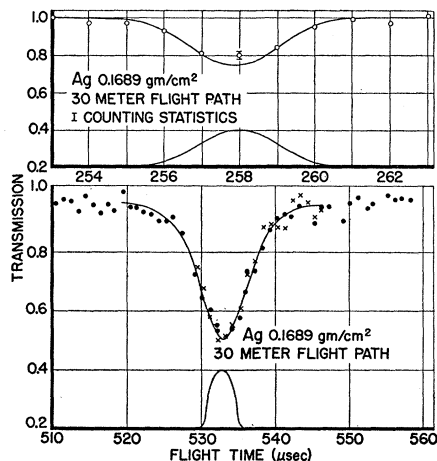


FIG. 4. Transmission of a thin Ag sample at the 72-ev (top curve) and the 16-ev resonances. The points and crosses are experimental data, and the solid curves were obtained by convoluting the calculated resolution function (under each transmission curve) with a calculated transmission obtained from the resonance parameters given in Table I. In the top curve, the resolution function used gives a good fit to the points on the sides of the resonance.

Procedures for relating measured areas to the Breit-Wigner (BW) resonance parameters, including Doppler broadening temperature effects, are discussed by Melkonian *et al.*³ and Seidl *et al.*¹ The two methods which have been used here are more recent developments which are felt to be simpler and quicker.^{6,14}

Since $g\Gamma_n = \sigma_0\Gamma/4\pi\lambda_0^2$, the value of $\sigma_0\Gamma$ is primarily desired from these measurements. One method used is designed to give $\sigma_0\Gamma$ directly,¹⁴ and if the sample is thin, the value obtained is relatively independent of the actual value of Γ . Thus reasonable determinations of $g\Gamma_n$ can be made without knowing Γ_γ accurately.⁶

For a single thin-sample resonance determination, Γ_γ is assumed to have a value determined from the average of other resonances where Γ_γ has been determined. If Γ_n is found to be comparable to Γ_γ , reiteration can be used to determine the best value for $\sigma_0\Gamma$. The average Γ_γ 's are also used in this paper where single thickness samples were measured. In most cases thick-thin samples are available and the data are presented as determined, but they can be readily reinterpreted in terms of the average Γ_γ where the accuracy of the data may indicate a preference.

Fairly accurate measurements of level widths are made in the 0-10 ev energy region by both crystal spectrometers and fast choppers where the level widths are large compared to the instrument resolution. Reasonably accurate values can also be determined for strong, well isolated resonances by area methods, and if this information is not available, extrapolated values

¹⁴ D. J. Hughes, J. Nuclear Energy 1, No. 4, 237 (1955).

are used from curves showing the Γ_γ width as a function of the atomic number.¹⁵

Multiple reiteration procedures are often desirable in obtaining a relation between an area and the BW parameters since the corrections imply a knowledge of the resonance. The situation becomes more complicated when the effects of several resonances must be taken into account. Cases exist in Ta in which the effect of a very strong resonance appears to influence a large energy region covering many other resonances.

In calculating the BW parameters, the following procedures were used in order to make the necessary corrections.

(1) The original base line was drawn between regions where the transmission is varying slowly between resonances. In most cases this could be drawn to equal valued and constant transmissions on both sides of the resonance. If not, the base line was tilted to follow any trends in the transmission. The area was measured between $E_0 + \Delta E$ and $E_0 - \Delta E$ in the usual manner.¹⁻³ Wing corrections were applied and the analysis made to determine $\sigma_0 \Gamma^P$, where P is a constant which is obtained from the area method with a value between 1 and 2. Reiterations were made where large wing corrections were involved or where an appreciable value for Γ_n was found. If thick-thin samples were available, the process could be done independently, but where only one sample was available an assumed average value of Γ_γ was required. Previous information about the level was used where possible.

(2) The effect of the resonance was calculated in the wings where the original base line was placed and the base line redrawn removing the effect of the resonance from the transmission. The area was remeasured and the analysis repeated if the area change was appreciable. If the interference term was appreciable, the area measurement involved a subtraction of the area below the base line from that above. Thus, the

interference term was assumed to have symmetrical contributions on both sides of the resonance except for sign.

(3) The steps outlined in procedures (1) and (2) were repeated until the values obtained converged. In any given case a single reiteration for any factor was usually sufficient and frequently the various factors could be included in a single reanalysis. For some well-isolated resonances the base line could be drawn far enough away that reiteration was not required, but for other cases it was necessary to re-examine the data using several resonances before final results were found.

By the foregoing approach, effects of adjacent resonances are automatically included in the base. As a check upon the method, the potential scattering, σ_p , has been calculated for the energies between the resonances for the cases in which the cross-section values appear to be resolved and Doppler effects can be neglected. If the potential scattering was found to be reasonably constant, it was interpreted as confirmation that the base was properly drawn. Unfortunately, a general procedure does not appear to be feasible in correcting for adjacent resonances, and strong resonances appear to require special attention to obtain the best interpretation of the data.

To determine σ_p , corrections for the resonance parts of the BW formula were made in two manners. First, sets of values at each energy were derived for adjacent resonances only. Second, corrections were made including all known resonances with measured parameters and including other resonances by using average parameters and the average level spacing in a series approximation. Thus, two procedures were followed to see if a choice existed.

The approach of correcting for all resonances will not work for the interference term because of the divergence of the interference series using average parameters needed to account for unmeasured resonances. The value of the interference due to all higher and lower energy resonances is indeterminant. Therefore, interference corrections were made only for the two adjacent resonances, and the assumption was made that positive and negative effects would cancel out on the average if enough energy points were included. In the case of strong resonances, corrections were made symmetrically on both sides until the contributions were negligible. The transmissions and total cross-section curves were used as guides as to the need of correction for a given resonance.

The above procedure also yields a value of σ_p which is of interest because of its relation to the nuclear radius. This measurement was not included in the original objective, and therefore, optimum sample thicknesses were not used. A measure of σ_p by this method will not be extremely sensitive unless regions are found where the resonances have little effect. Approximate initial values of σ_p' must be used to correct for the resonances,

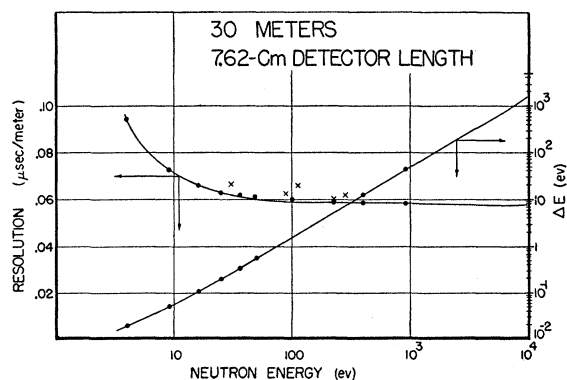


FIG. 5. The calculated resolution (full width at half-maximum in $\mu\text{sec}/\text{meter}$ and energy uncertainty) as a function of energy. Experimental values are given by crosses.

¹⁵ H. H. Landon, Phys. Rev. **100**, 1414 (1955); J. S. Levin and D. H. Hughes, Phys. Rev. **101**, 1328 (1956).

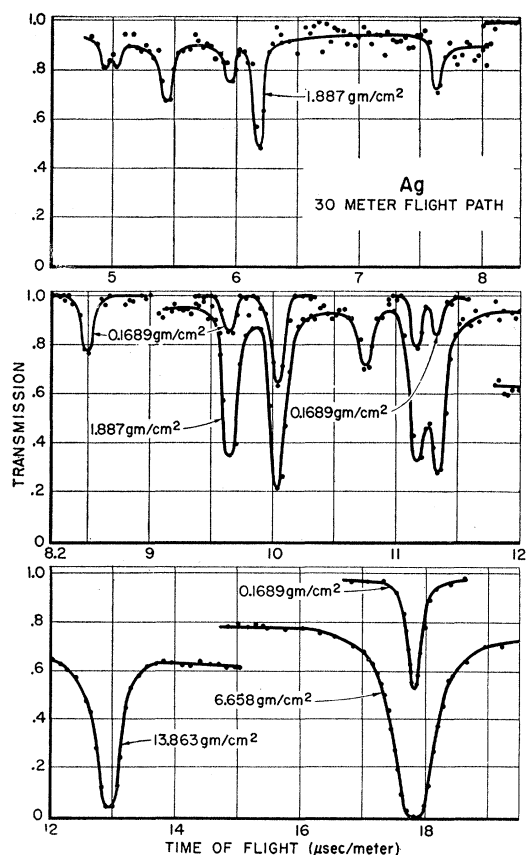


FIG. 6. Experimental transmission curves for normal Ag. The solid lines are visual averages and are representative of those used for the area analyses of the resonances.

and the final σ_p must be approached by a reiteration procedure.

V. RESULTS

Silver

A fairly extensive series of measurements has been made using normal silver. Resolutions used varied from 0.17 to 0.05 $\mu\text{sec}/\text{meter}$. The samples had a purity of 99.9%, and the isotopic assignments of resonances are those given by Seidl.¹ Typical transmission curves are shown in Fig. 6.

TABLE II. A summary of the average parameters for Ag as obtained at BNL¹ and at MTR. The values $\bar{\Gamma}_n^0/D$ for the individual isotopes are the actual ratios of $\bar{\Gamma}_n^0$ to D , while $[\bar{\Gamma}_n^0/D]$ for the element is obtained by the method given in Fig. 8.

	Ag ¹⁰⁷		Ag ¹⁰⁹	
	MTR	BNL	MTR	BNL
Γ_γ (mv)	135 \pm 17	130	134 \pm 40	130
$\bar{\Gamma}_n^0$ (mv)	1.5 \pm 0.6	2.1	2.8 \pm 0.8	3.0
D (ev)	38 \pm 6	50	34 \pm 3	33
$(\bar{\Gamma}_n^0/D) \times 10^4$	0.40 \pm 0.16	0.16	0.82 \pm 0.4	0.91
Average $\bar{\Gamma}_n^0/D$ for element = $(0.61 \pm 0.2) \times 10^{-4}$.				
Average $[\bar{\Gamma}_n^0/D]$ for element = $(0.54 \pm 0.2) \times 10^4$.				

A summary of the derived parameter values is given in Table I. The average level spacing reported in Table II was obtained by averaging the known level spacings and using estimated values for the upper and lower limit spacings. For Ag¹⁰⁹ the lower limit spacing was estimated to be 2×5.2 ev, and the upper spacing was taken as $(136 - 90)/2$ ev. Correspondingly, values of $(136 - 52)/2$ and $(16 + 5)$ ev were assumed for the upper and lower spacings for Ag¹⁰⁷. Information about the 5.2-ev level in Ag¹⁰⁹ was used from crystal spectrometer measurements of Wood.¹⁶ In Wood's work a negative level between -1 and -10 ev is proposed, and this evidence forms the basis of the lower spacings quoted above.

A plot of the number of resonances below energy E for normal Ag as a function of energy is shown in Fig. 7. Since levels are being missed above 90 ev, $\bar{\Gamma}_n^0$ and D are based on the averages of the resonances below this energy in Table I. The deviations for the average values, $\bar{\Gamma}_n^0$ and D , are deviations of the mean

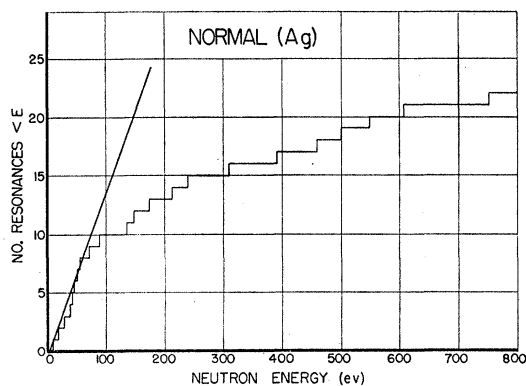


FIG. 7. The number of resonances below the energy E as a function of energy for normal Ag. This curve indicates that resonances are definitely being missed above 90 ev.

obtained from the mean square deviations of the individual values. For the average absorption width, $\bar{\Gamma}_\gamma$, each value has been weighted according to the accuracy of the determination so the 5.2-ev level value dominates the Ag¹⁰⁹ average. Although the individual values of Γ_γ show fairly wide deviations, the accuracy does not conflict with the assumption that Γ_γ is constant for each level. The Γ_γ for the 72-ev level is low, but if the BNL¹ thick sample area is combined with the MTR thin sample area, a value of 145 ± 55 mv results.

The sum of the Γ_n^0 's up to energy E as a function of E is plotted in Fig. 8 for both isotopes. The slope should give $4 \times [\bar{\Gamma}_n^0/D]$ ¹⁷ where in this case $[\bar{\Gamma}_n^0/D]$ is an average for the two isotopes of the element since the 2 isotopes (each with 2 spin states) have almost equal

¹⁶ R. E. Wood (private communication).

¹⁷ The use of square brackets around $\bar{\Gamma}_n^0/D$, $[\bar{\Gamma}_n^0/D]$, is intended to imply that the average has been determined from the curve of $\Sigma \Gamma_n^0$ vs energy.

abundance. Since thick samples have been used above 90 ev where the resonances were not resolved, the low-energy points have been weighted heavily in determining the slope. If the resonances are not single, the Γ_n^0 values would be too large ($A^2 \propto \sigma_0 \Gamma^2$). The reciprocal of the statistical factor, $1/g$, is assumed to be 2 except where a preference is indicated.

Table II is a summary of the parameters as obtained here and at BNL. The differences between MTR and BNL averages are primarily due to the choice made in determining D , the use of preferred values of g , and disagreement on the parameters for the 72-ev level. It is seen that the limited number of levels measured allows considerable latitude in the procedure resulting in additional uncertainty about the final value. The average $[\bar{\Gamma}_n^0/D]$ for the two isotopes or the element indicates that the Ag¹⁰⁹ value may be high. All values are within the errors so that significant changes are not justified without higher resolution information and more levels. A recently reported¹⁸ technique, which averages

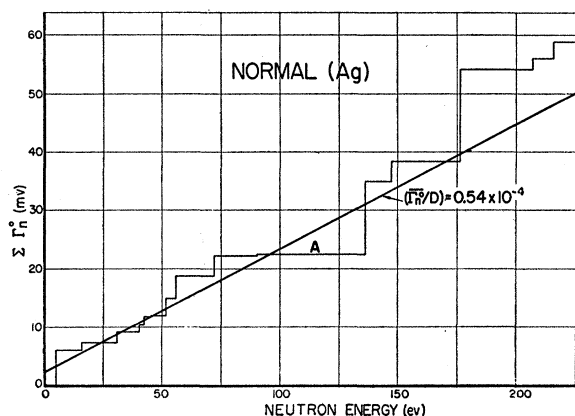


FIG. 8. The sum of the Γ_n^0 's found up to the energy E as a function of E for normal Ag.

many levels, gives $\bar{\Gamma}_n^0/D$ for the element Ag as $(0.3 \pm 0.1) \times 10^{-4}$.

To calculate the potential scattering between levels, an initial value of the potential scattering must be assumed. For this purpose initial values, indicated by primes, of $\sigma_p'(107) = 7.3$ barns and $\sigma_p'(109) = 4.7$ barns as given by Wood (the average is quoted as 6.0 ± 0.5 barns) have been used. The various values obtained and the average are summarized in Table III. Since the data were not reiterated to give a best fit of σ_p , the final value is not independent of the initial σ_p' values used. Reiteration is indicated by the large difference between the final and initial values, but the absolute accuracy of the total cross sections does not justify it. The absolute error is indicated in the final result quoted.

The primary interest was to observe the constancy of σ_p as a measure of the validity of the methods used

TABLE III. The average potential scattering calculations for Ag at energies between resonances with assumed values $\sigma_p'(107) = 7.3$ barns, $\sigma_p'(109) = 4.7$ barns.

E (ev)	σ_t (barns)	σ_p (barns)	Summary of σ_p from column 3
23.7	5.8	5.5	Average $\sigma_p = 5.1$ barns.
35.7	6.0	5.3	Deviation of individual
41.6	not resolved		values = 0.5 barn. Deviation
43.8	8.6	4.8	of mean = 0.1 barn.
48.7	5.7	5.5	The best value is $\sigma_p = 5.1$
54.1	13.0	4.1	± 1 barns, with the error
64.15	5.7	5.6	including an estimate of
80.9	5.9	5.2	accuracy.

in the analysis. Aside from the value at 54 ev, which is two standard deviations from the mean, the individual values are constant within the accuracy expected from the parameters. The most consistent set was found by correcting for the adjacent resonances only, but this was very insensitive in the case of the resonance term. The calculated value of σ_p from the equation,

$$\sigma_p = 4\pi(1.45A^{1/3} \times 10^{-13})^2,$$

is 6.0 barns.

Tantalum

Table IV summarizes the resonance parameters for Ta¹⁸¹. The resonances at 56, 85, 89, 136, and 147 ev have been reported,¹⁹ and the fact that two sets of levels exist in the 23- and 35-ev regions were discovered in this investigation.^{6,19} The 4.3- and 10.4-ev resonance parameters have been taken from the literature.^{6,16} Other work on tantalum in a corresponding energy region has been done,^{3,20,21} but the results here are more nearly in agreement with those given by Harvey *et al.*⁶ It is to be noted that the individual values of Γ_n appear to be remarkably constant. Strong levels at 39 and 99 ev are worthy of special note.

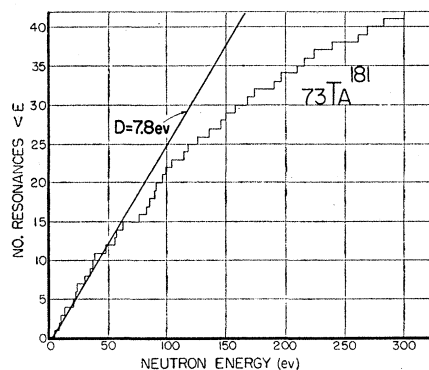


FIG. 9. The number of resonances below the energy E as a function of energy for Ta. The average level spacing per spin state, D , is twice the reciprocal slope of the straight line shown. This curve indicates that levels are being missed above 65 ev.

¹⁹ Simpson, Fluharty, and Simpson, Phys. Rev. **99**, 610(A) (1955).

²⁰ R. L. Christensen, Phys. Rev. **92**, 1509 (1953).

²¹ Gaertner, Yeater, and Albert, U. S. Atomic Energy Commission Report KAPL-1084, 1954 (unpublished).

¹⁸ D. J. Hughes and V. E. Pilcher, Phys. Rev. **100**, 1249(A) (1955).

TABLE IV. Parameters for resonances measured in Ta¹⁸¹ by MTR fast chopper. The $1/g$ factor is assumed to be 2, and Δ is the Doppler width of the level. Errors on individual parameters are estimates of accuracy and are about 3 times as large as the precision associated with the measurements. $\bar{\Gamma}_n^0 = 1.88 \pm 0.3$ mv; $D = 7.8 \pm 2$ ev; $\bar{\Gamma}_n^0/D = (1.7 \pm 0.3) \times 10^{-4}$; $\bar{\Gamma}_\gamma = 49 \pm 3$ mv.

E_0 (ev)	$(1/n) \times 10^{24}$ cm ² /atom	Δ (ev)	Area (ev)	$\sigma_0 \Gamma$ (b-ev)	σ_0 (kb)	$g \Gamma_n$ (mv)	Γ_γ (mv)	Γ_n^0 (mv)
14.0±0.15	35.83	0.093	0.743±0.030	104±15	2.2±0.9	0.56±0.006	48±15	0.30±0.06
	1356		0.103±0.009					
20.5±0.2	35.83	0.113	0.671±0.040	70±15	1.4±0.6	0.54±0.09	52±15	0.24±0.06
	1356		0.0725±0.0160					
22.9±0.3	35.83	0.119	0.357±0.064	14.6±3.3		0.13±0.03		0.054±0.012
24.3±0.3	235.0	0.123	0.703±0.084	410±60	7.1±3.3	3.8±0.6	50±24	1.56±0.24
			0.309±0.034					
29.5±0.3	35.83	0.136	0.338±0.046	12.1±2.4		0.14±0.03		0.05±0.012
35.3±0.6	4655	0.149	0.156±0.031	473±78		6.4±1.5		2.32±0.54
36.1±0.6	4655	0.150	0.181±0.036	560±93		7.7±1.2		2.58±0.42
39.3±0.6	235.0	0.156	1.555±0.233	1755±350	19.1±6.9	26±6	40±30	8.4±1.8
	4655		0.365±0.051					
49.2±0.7	235.0	0.17	0.198±0.044	35.4±8.9		0.66±0.16		0.188±0.047
55.9±0.8	35.8	0.17	0.145±0.072	4.4±2.2		0.1±0.05		0.027±0.013
57.9±0.8	35.8	0.18	0.145±0.072	4.4±2.2		0.1±0.05		0.027±0.013
63.2±0.9	235.0	0.19	0.533±0.120	150±35		3.6±0.9		0.91±0.23
76.9±1.2	235.0	0.21	1.121±0.280	729±182		2.1±5.0		4.8±1.14
82.7±1.4	235.0	0.22	0.651±0.228	176±62		5.5±2.0		1.21±0.44
84.7±1.4	235.0	0.22	0.298±0.135	56±28		1.8±0.9		0.39±0.19
89.4±1.9	235.0	0.23	0.345±0.170	66±33		2.2±1.1		0.47±0.23
91.4±1.9	235.0	0.23	0.171±0.085	29±15		1.0±0.5		0.21±0.11
98.8±2.0	235.0	0.24	2.32±0.46	1880±376		71±14		14.3±0.28
105±2.0	235.0	0.25	0.971±0.240	410±103		17±4		3.22±0.78
114±2.0	235.0	0.26	1.29±0.36	694±208		30±9		5.6±1.69
125±3.0	235.0	0.27	1.11±0.27	470±118		23±7		4.02±1.07
136±3.0	235.0	0.28	1.34±0.33	658±165		34±9		5.84±1.46
147±3.0	235.0	0.29	0.586±0.20	137±4.8		7.5±3.0		1.24±0.44

A plot of the number of resonances with an energy less than E as a function of E is given in Fig. 9, and the value of D indicated is 7.8 ± 2 ev per spin state. If the size distribution for Γ_n^0 is assumed to be exponential,⁶ the slope of the integral distribution curve gives $\bar{\Gamma}_n^0 = 1.88 \pm 0.3$ mv for the levels below 65 ev. The ratio obtained from these values is $\bar{\Gamma}_n^0/D = 2.4 \times 10^{-4}$.

A plot of the sum of Γ_n^0 's up to E as a function of energy is shown in Fig. 10. Line C has been chosen as the best choice which gives $[\bar{\Gamma}_n^0/D] = (1.7 \pm 0.3) \times 10^{-4}$. This value agrees well with the value 1.8×10^{-4} which has been reported previously.¹⁸ The other lines drawn represent possible interpretations that are considered much less likely. Line A has a slope con-

sistent with the value of $\bar{\Gamma}_n^0/D$ given above from $\bar{\Gamma}_n^0$ and D , and is clearly too high. Line B is also considered high since the samples used for the high-energy resonances were not truly thin. Line D is considered to be low since it fails to give sufficient weight to the large resonances. Lines B and D are selected as limits for the preferred curve C .

From the discrepancy between curves A and C , arrived at by different approaches from the same data, it would appear likely that the interpretation of the size distribution curve placed undue weight upon strong resonances. And as an isolated case, this isotope does not show good agreement with an exponential distribution for the number of levels investigated. Also the foregoing arguments indicate that weak levels are possibly being missed. Higher resolution measurements with a larger number of levels are indicated before such conclusions are given great significance.

The potential scattering calculations for Ta at energies between resonances are given in Table V. The statistical variations correcting only for adjacent resonances demonstrate the need for including the effect of resonances several spacings away. In particular, corrections are needed for the 39-, 36-, and 35-ev resonances. Reiteration using the derived σ_p does not improve the constancy of σ_p or change its value. It is quite likely that the analysis assumptions do not fit this case precisely or that the errors are slightly larger than predicted since the expected precision is smaller than the observed spread in σ_p values. The agreement is considered to be satisfactory for the purposes of

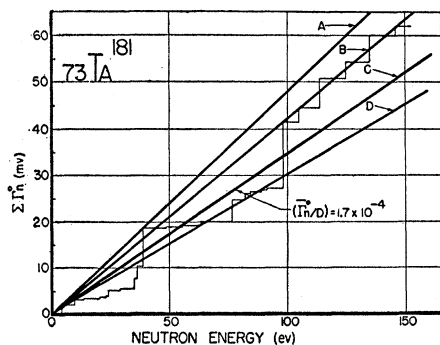


FIG. 10. The sum of the Γ_n^0 's observed up to the energy E as a function of E for Ta. Curve A has a slope which agrees with the value of $\bar{\Gamma}_n^0/D$ obtained from the arithmetic average values of $\bar{\Gamma}_n^0$ and D . The preferred value (see discussion on Ag) is given by curve C with limits given by curves B and D .

TABLE V. The potential scattering calculations for Ta at energies between resonances. Corrections are made for the 39-, 36-, and 35-ev resonances several resonances away from E_0 .

E (ev)	σ_t (barns)	σ_p (barns)	Summary of σ_p from column 3
16.5	9.7	9.5	Average $\sigma_p=9.1$ barns. Deviation of individual values $=\pm 0.6$ barn. Deviation of the mean $=0.25$ barn. The best value is $\sigma_p=9.1\pm 1$ barns, with the error including an estimate of the accuracy.
18	8.8	8.8	
22	8.1	8.5	
23.4	not resolved		
27	8.3	8.0	
32	7.1	9.2	
37.7	not resolved		
46.5	13.8	9.9	
54	11.0	9.6	

obtaining averages. The data presented here show no preference as to whether the correction for the resonance term in the Breit-Wigner formulas include only adjacent or all resonances. The potential scattering obtained using $4\pi R^2$ with $R=1.45\times 10^{-13}$ A^{1/2} is 8.5 barns which is in good agreement with the value in the table. Wood¹⁶ reports 7.0 ± 1 barns.

Uranium-238

The uranium measurements have been made with a resolution of 0.1 μ sec/meter, and a summary of the analysis is given in Table VI. Harvey *et al.*,⁶ using 0.07 μ sec/meter, reports levels at 90 (very weak), 146, and 166 which are not seen in these results. Also, other levels up to 418 ev are reported. Aside from these differences which can be attributed to the differences in resolution used, the agreement is excellent. Also the agreement with other measurements made with the fast chopper at the Argonne National Laboratory is good.²²

Average values of the observed spacings and scattering widths have been used analogous to the treatment used for Table I for Ag since the number of levels are

limited, and statistical methods did not appear advisable. Information for the 6.7-ev level has been used from work by Levin and Hughes.¹⁵

VI. CONCLUSIONS

The data presented show that the MTR chopper results are in agreement with other chopper measurements. The resolution of 0.05 to 0.17 μ sec/meter is demonstrated by the splitting of the 42.4- and 45.2-ev levels in Ag and by the discovering of additional levels in Ta.

A method for determining potential scattering between resonances is indicated for Ag and Ta. The procedure has been used here primarily as a check upon analysis methods, but the values obtained for σ_p are of interest as well. Corrections are required for adjacent resonances and, in some cases, for large resonances several level separations away.

VII. ACKNOWLEDGMENTS

The authors wish to acknowledge the valuable contributions made by many persons throughout the planning, installation, and preliminary runs of the MTR fast chopper. The planning, motivation, and guidance provided by R. L. Doan, F. W. Crawford, and J. E. Evans have been necessary to the program. We are grateful to R. Sliger for design, testing, and installation of the chopper assembly; to H. Watanabe for design of the collimation system; to R. E. Heffner and R. O. Lambert for fabrication and installation of mechanical units of the system; to D. R. deBoisblanc and other members of the MTR Instrument Development Section for the design, construction, and maintenance of the time-of-flight and rotor speed control circuitry; and to the MTR Operating Personnel who have monitored chopper performance on a 24-hour

TABLE VI. Parameters for resonances measured in U²³⁸ by MTR fast chopper. The $1/g$ factor is assumed to be 1, and Δ is the Doppler width of the level. Errors on individual parameters are estimates of accuracy and are about 3 times as large as the precision associated with the measurements.

E_0 (ev)	$(1/n)\times 10^{24}$ cm ² /atom	Δ (ev)	Area (ev)	$\sigma_0\Gamma$ (b-ev)	σ_0 (kb)	$g\Gamma_n$ (mv)	Γ_γ (mv)	Γ_n^0 (mv)
21.2 \pm 0.3	307 10639	0.096	0.768 \pm 0.108 0.146 \pm 0.028	1266 \pm 250	35.0 \pm 13	10.3 \pm 2.0	25.9 \pm 12.0	2.2 \pm 0.8
37.0 \pm 0.6	460.5 10639	0.125	1.087 \pm 0.076 0.254 \pm 0.056	2310 \pm 670	38.4 \pm 18	32.6 \pm 9.0	27.7 \pm 24.0	5.35 \pm 3.2
66.0 \pm 2.5	460.5 2460	0.169	0.858 \pm 0.051 0.413 \pm 0.054	1005 \pm 220	15.6 \pm 7.0	25.4 \pm 7.0	39.1 \pm 26	3.1 \pm 2.0
80.2 \pm 2.0	460.5	0.188	0.209 \pm 0.050	76.5 \pm 22		2.34 \pm 0.8		0.26 \pm 0.16
101 \pm 3.0	460.5	0.212	1.27 \pm 0.102 0.636 \pm 0.095	1786 \pm 500	19.2 \pm 11.0	69.0 \pm 20.0	24.0 \pm 26.0	6.85 \pm 4.0
115 \pm 3.5	460.5	0.223	0.603 \pm 0.084	317 \pm 84		14.0 \pm 4.0		1.3 \pm 0.8
181 \pm 7.0	307	0.28	2.87 \pm 0.40	2235 \pm 560		155 \pm 40		23.0 \pm 6
200 \pm 8.0	307	0.294	2.62 \pm 0.47	1940 \pm 600		148 \pm 46		21 \pm 7
$\bar{\Gamma}_\gamma = 29.3\pm 10.0$ mv; $\bar{\Gamma}_n^0 = 2.8\pm 0.9$ mv; $D = 18\pm 2$ ev; $\bar{\Gamma}_n^0/D = (1.55\pm 0.5)\times 10^{-4}$.								

²² Bollinger, Cote, Dahlberg, and Thomas (private communication, 1955).

schedule, recorded data, and changed samples. We acknowledge the assistance of M. S. Smith and S. S. Allison for assistance in processing data. We have had free access to the fast chopper and cross-section

experience at the Argonne National Laboratory, Columbia University, and the Brookhaven National Laboratory. The latter laboratory should be thanked in particular for constructing the chopper rotor.

Nuclear Moments of Inertia due to Nucleon Motion in a Rotating Well*

D. R. INGLIS

Argonne National Laboratory, Lemont, Illinois

(Received May 31, 1956)

A model of a deformed nucleus in which the spheroidal collective field is steadily cranked about a fixed axis, as introduced in previous papers, serves as a convenient approximation expected to reproduce some of the dynamic inertial properties of the collective motion. The independent-nucleon behavior in a rotating harmonic oscillator potential, deformed by the presence of the open-shell nucleons, gives the rigid-rotation moment of inertia and is discussed here with an attempt at graphic clarity. This result is much larger than observed and attention is here focused on the shortcomings of the harmonic oscillator approximation, although, as suggested by Bohr and Mottelson, the discrepancy may also be largely due to the internucleon interactions which have not been calculated adequately and are here neglected. The $1d-2s$ shell is treated as a tractable illustrative case. The characteristic harmonic-oscillator degeneracy of the undeformed levels within the magic-number groups, such as the $1d$ and $2s$ levels, profoundly affects the perturbation calculation of the moment of inertia through the energy denominators. Removing this degeneracy by lowering the states of high l (as required in heavier nuclei for the magic numbers) has the effect of increasing the calculated moment of inertia above the rigid-rotation value in most cases near the beginning of the shell and reducing it in most cases near the end of the shell. The preponderance of prolate deformations is also discussed.

THE effective moment of inertia of a distorted nucleus may conveniently be investigated by constraining the fictitious potential (first approximation to a self-consistent field) defining the wave functions to rotate with constant angular velocity Ω about a fixed axis in space.¹ This procedure gives a rotational angular momentum of the form¹

$$\hbar\langle L_x \rangle_0 = \Omega \hbar^2 \sum_i | \langle i | L_x | 0 \rangle |^2 / (E_0^{(0)} - E_i^{(0)}), \quad (1)$$

arising from the admixture of excited states i in a perturbation theory by a relatively small Coriolis term $-\hbar L_x \Omega$ in the Hamiltonian. The essential approximation in this model is the neglect of "recoil" fluctuations in the angular velocity of the distorted effective potential contributed by the collective behavior of the many nucleons, leaving the angular momentum not strictly a constant of the motion. This may be accepted as an alternative to the approximation involved in assuming the "interaction" or "fluctuations" to be small in other treatments which in other manners formulate the separation of the internal and collective aspects of the motion.²⁻⁴

* Work performed under the auspices of the U. S. Atomic Energy Commission.

¹ D. R. Inglis, Phys. Rev. **96**, 1059 (1954). *Erratum*: For a correction in the method of deriving the expression for the rotational energy, see Appendix.

² A. Bohr and B. R. Mottelson, Kgl. Danske Videnskab. Selskab, Mat.-fys. Medd. **30**, No. 1 (1955). See also S. A. Moszkowski, Phys. Rev. **103**, 1328 (1956); G. Lüders (to be published).

³ A. Bohr, Kgl. Danske Videnskab. Selskab, Mat.-fys. Medd. **26**, No. 14 (1952); *Rotational States of Atomic Nuclei* (E. Munsgaards Forlag, Copenhagen, 1954).

Early calculations^{1,2} with this model have employed three-dimensional harmonic oscillator potentials and wave functions, elongated or flattened along an axis perpendicular to the axis of rotation. The method was first applied to artificially distorted closed-shell nuclei, and it was shown¹ that the closed-shell nucleons in this approximation contribute only the small moment of inertia characteristic of irrotational fluid flow.³ In actual nuclei the distortion is due to the presence of additional open-shell nucleons and the observed moments of inertia are, in most cases, about five times that large so it appeared on this basis that the closed-shell nucleons contribute much less than their proportionate share of the moment of inertia.

Extending the treatment to include the contribution of open-shell nucleons, Bohr and Mottelson² (without pausing to present an explicit derivation, which is indeed quite simple, as we shall see) give the very interesting expression for the moment of inertia

$$\mathcal{I}_x = \frac{\hbar}{2\omega_2\omega_3} \left\{ \frac{(\omega_2 - \omega_3)^2}{\omega_2 + \omega_3} \sum (m+n+1) + \frac{(\omega_2 + \omega_3)^2}{\omega_2 - \omega_3} \sum (n-m) \right\}. \quad (2)$$

⁴ H. A. Tolhoek, Physica **21**, 1 (1955); F. Coester, Phys. Rev. **99**, 170 (1955); Bull. Am. Phys. Soc. Ser. II, **1**, 194 (1956); Lipkin, de-Shalit, and Talmi, Nuovo cimento **2**, 773 (1955); S. Tomonaga, Progr. Theoret. Phys. Japan **13**, 467 (1955); F. Villars (to be published). The related vibration problem is treated by J. M. Araujo, Nuclear Phys. **1**, 259 (1956).